ASTRONOMY & ASTROPHYSICS
SUPPLEMENT SERIES

NOVEMBER II **1994**, PAGE 73

Astron. Astrophys. Suppl. Ser. **108**, 73-78 (1994)

Optical nebulosities associated with IRAS sources in dense cloud cores

C. Eiroa[1], J.M. Torrelles[2], L.F. Miranda[3], G. Anglada[4] and R. Estalella[4]

[1] Dpto. Física Teórica C-XI, Facultad de Ciencias, Universidad Autónoma de Madrid, Cantoblanco, E-28049 Madrid, Spain
[2] Instituto de Astrofísica de Andalucía, CSIC, Apdo. Correos 2144, E-18080 Granada, Spain
[3] Dpto. Astrofísica, Facultad de Ciencias Física, Universidad Complutense de Madrid, E-28040 Madrid, Spain
[4] Departament d'Astronomia i Meteorologia, Universitat de Barcelona, Av. Diagonal 647, E-08028 Barcelona, Spain; and Laboratori d'Astrofisica, Societat Catalana de Fisica, IEC, Spain

Received January 12; accepted May 17, 1994

Abstract. — I, Hα and [SII] CCD images of the regions around 4 young IRAS sources embedded in the dense molecular cloud cores CB 6, CB 39, AFGL 5142, and L 1251 are presented. Reflection nebulosities are found in all 4 regions. Herbig-Haro objects are detected in AFGL 5142 and L 1251. In both cases, the HH objects are new discoveries.

Key words: stars: pre-main sequence — ISM: jets and outflows — reflection nebulae

1. Introduction

It is well established that dense cores in molecular clouds are sites of recent star formation. The IRAS satellite revealed a huge number of sources embedded in cloud cores, which were identified as recently formed stellar objects (e.g. Beichman et al. 1986). These pre-main sequence objects experience energetic mass loss processes in their earliest evolution, which are observed in a large variety of ways. At optical wavelengths the outflows are detected as cometary and bipolar reflection nebulosities and shock-excited Herbig-Haro objects. Deep, sensitive CCD images taken through continuum and emission line filters constitute an efficient way of detecting the optical outflows from young stars and, in addition, allow us to distinguish between reflection nebulosities and Herbig-Haro objects (e.g. Hartigan & Lada 1985).

In this work we present the results of several observational campaigns carried out at the Observatories of Calar Alto and La Palma, where we obtained CCD images of the fields around several young IRAS sources embedded in dense cores. In some cases, AFGL 5157, S 140N, L 1448 and L 1527, the results have already been published (Torrelles et al. 1992a; Eiroa et al. 1993, 1994). In some other cases, L 723, L 778 and the field around IRAS 22343+7501 in L 1251, our images confirm previous published observations. The rest of the cores, CB 6, CB 39, AFGL 5142, and the field around IRAS 22376+7455 in L 1251, are presented here. Table 1 gives the equatorial coordinates and fluxes of 4 IRAS young stellar sources located in these cores; their positions are approximately the center of our images. Reflection nebulosities and/or Herbig-Haro objects are detected in all cases.

2. Observations

CCD images were taken during 1989 and 1990 at Calar Alto (Almera) and Roque de Los Muchachos (Canary Islands) Observatories. On Calar Alto we used the 3.5 m telescope equipped with a CCD camera, chip RCA 624×1024 pixels and pixel size 15 μm, installed at its prime focus. The scale on the focal plane is $0\farcs2535$/pixel. Images were obtained with a broad-band filter I ($\lambda \approx$0.9 μm) and interference filters Hα ($\lambda \approx$6580 Å, FWHM$\approx$100 Å), [SII] ($\lambda \approx$6740 Å, FWHM$\approx$70 Å) and red continuum r_n ($\lambda \approx$7200 Å, FWHM$\approx$800 Å). On Roque de Los Muchachos we used the 2.5 m INT; these observations were carried out using a 385×578 pixel GEC CCD detector, pixel size 22 μm, at the telescope prime focus. The scale on the focal plane is $0\farcs54$/pixel. A broad-band I filter ($\lambda \approx$0. 9 μm) and interference filters Hα ($\lambda \approx$6569 Å, FWHM$\approx$60 Å) and [SII] ($\lambda \approx$6730 Å, FWHM$\approx$48 Å) were used. A log of the observations is presented in Table 2, where dates, exposure times and seeing conditions are given. Flat field correction and dark subtraction of each object frame have been made following standard procedures. In addition, the images have been astrometrically calibrated by means of a

Table 1. IRAS sources associated with the cloud cores

IRAS	CORE	RA (1950)			DEC (1950)			Flux density (Jy)			
		h	m	s	°	′	″	[12]	[25]	[60]	[100]
00465+5028	CB6	00	46	34.3	50	28	25	0.25L	1.01	3.96	8.96
05274+3345	GL5142	5	27	27.6	33	45	37	6.89	69.36	449.32	905.75
05591+1630	CB39	5	59	6.0	16	30	58	4.53	9.87	7.27	10.64
22376+7455	L1251	22	37	40.8	74	55	50	0.8	5.6	32.0	66.0

Table 2. Log of observations

Object	Telesc	Date	Filter	Exp time	Seeing
CB 6	2	27.11.89	I	900	2″
			Hα	1800	*
			[SII]	1800	*
GL5142	1	17.11.89	I	900	1.″5
			Hα	1800	1.″5
			[SII]	900	1.″5
	1	30.10.90	I	900	1.″2
			Hα	1800	1.″2
			[SII]	1800	1″
	2	27.11.89	I	300	2″
CB39	2	29.11.89	I	30	2″
			Hα	60	2″
			[SII]	60	2″
IRAS 22376	2	30.11.89	I	600	2.″2
			Hα	900	2.″2
			[SII]	900	2.″2
	1	29.10.90	Hα	1800	2″
			[SII]	1800	2″

Telescope: (1) 3.5 m
Calar Alto, (2) 2.5 m INT

(*) Unfocussed due to technical problems

grid of SAO stars measured on Palomar Plates. Estimated position errors are 1.″5.

3. Results on individual objects

3.1. *CB 6*

CB 6 (LBN 613) is a small molecular core of ≈9′×3.′4 in size and position angle of 50° (Clemens & Barvainis 1988). The temperature and CO line width indicate that it is a cold, quiescent core. CB 6 is associated with an elongated bright rim of nebulosity visible on P.O.S.S. The highest obscuration is found at the northwestern end of this rim and has a fairly round shape with a small, compact nebulosity in its center. The source IRAS 00465+5028 is associated with CB 6 and has colours typical of young IRAS sources embedded in cloud cores (Clemens & Barvainis 1988; Beichman et al. 1986).

CCD images of CB 6 were taken at the INT. Figure 1 is an I-contour plot of the central part of CB 6 where the compact nebulosity is located. The first contour shows the background produced by the elongated bright rim. The compact nebulosity appears similar in the interference filters, suggesting that it is a pure reflection nebulosity. The position of IRAS 00465+5028 is marked in Fig. 1. Posi-

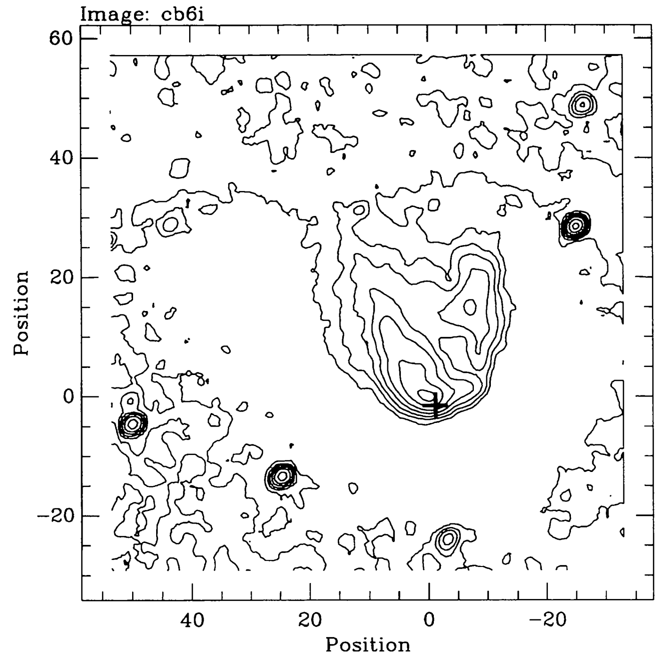

Fig. 1. I contour plot of CB 6. Axes are in arc seconds. Adjacent contours are separated by a factor $2^{1/2}$. Position (0,0) corresponds to the peak of the CB 6 nebulosity, Table 3. IRAS 00465+5028 is marked with a cross. North is up and east to the left. This convention is used throughout this paper

Table 3. Equatorial coordinates of stars and nebulosities embedded in the cores

Object	α(1950)			δ(1950)		
	h	m	s	°	′	″
CB6/I-peak	00	46	34.45	50	28	26.6
GL5142						
/star 1	05	27	28.10	33	45	39.6
/HH 190	05	27	27.54	33	45	38.4
CB39/star 1	05	58	47.66	16	29	55.3
IRAS 22376+7455						
/star 1	22	37	35.97	74	56	07.7
/star 2	22	37	37.32	74	55	48.8
/star 3	22	37	13.56	74	56	16.6
/HH 189A	22	37	34.14	74	55	14.6
/HH 189B	22	37	33.72	74	55	01.9
/HH 189C	22	37	33.10	74	54	10.0

tion (0,0) corresponds to the maximum of the nebulosity in the I filter; its 1950.0 coordinates are given in Table 3. The dark region around the nebulosity is clearly distinguished. IRAS 00465+5028 is located at the apex of the CB 6 reflection nebulosity. Morphologically, the object can be described as a cometary nebula illuminated by the young IRAS object.

3.2. *AFGL 5142*

AFGL 5142 (Price 1977) is a bright far-IR source listed in the IRAS Point Source Catalogue as IRAS 05274+3345, whose far-IR luminosity is 8.1 10^3 $L_{\odot}$, at an assumed distance of 1.8 kpc (Snell et al. 1988). Snell et al. detected a bipolar CO outflow, oriented east-west and approximately centred on the IRAS source. A high-density NH_3 core was mapped by Verdes-Montenegro et al. (1989), who also detected a H_2O maser in the region. A CS condensation similar to that in NH_3 has been observed by Pastor et al. (1991). Through higher angular resolution NH_3 observations Estalella et al. (1993) found that the high-density core is elongated in a direction perpendicular to the molecular outflow axis, and suggested that this may play a role in the collimation of the bipolar outflow. Torrelles et al. (1992b) refined the position of the H_2O maser and found a compact radio continuum source with a cometary-like morphology. Both the maser and the radio continuum source coincide with the NH_3 peak and are displaced ≈30″ east of the IRAS source. These authors suggest that the ionizing object of the radio continuum source drives the CO outflow in the region, although a contribution of IRAS 05274+3345 cannot be discarded.

Figure 2 shows a isocontour plot of the Calar Alto 1990 I image of the region. The positions of the IRAS and radio continuum sources are indicated in the plot. A cluster of red stars surrounded by a diffuse nebulosity is detected in the field. The most interesting object is a point-like stellar object, star 1 in Fig. 2 and Table 3, associated with a cometary-like reflection nebula oriented towards the west and slightly curved towards the south. The cometary nebula is oriented in the same direction as the blue lobe of the CO outflow. Detailed I, Hα and [SII] isocontour plots of the object are shown in Fig. 3. IRAS 05274+3345 is seen projected against the nebulosity and its nominal position is very close to a very red I star. With the present data, however, we cannot make a definitive association of the IRAS source with either this star or the star illuminating the nebulosity. A condensation located at 7″ west and 1.″2 south of star 1 is seen embedded in the reflection nebulosity, Fig. 3. This condensation is clearly detected in [SII] and Hα but not in the I image. Thus, this behaviour suggests that the condensation represents a site of HH emission, a fact which has recently been confirmed by an optical spectrum (E. Ortiz, private communication). We call this object HH 190, following the numbering of the HH object catalog by Reipurth (1994). Finally, we have not detected any object at the position of the radio source detected by Torrelles et al. (1992b).

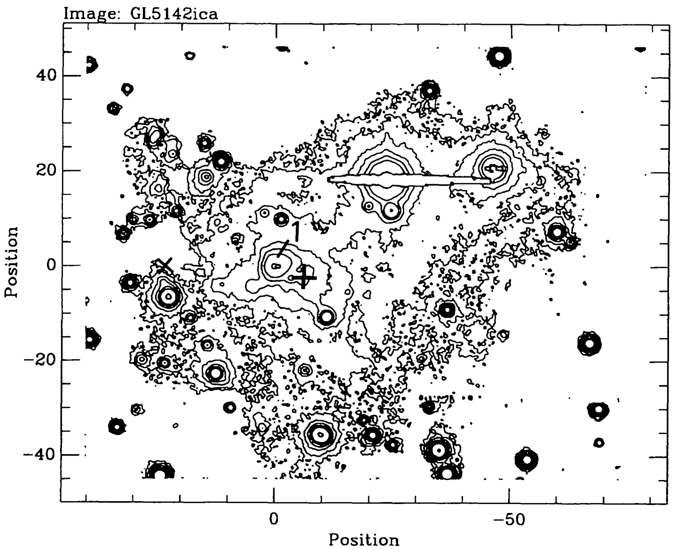

Fig. 2. I isocontours of the AFGL 5142 field. Axes are in arc seconds. First contour is 3σ and adjacent contours are separated by a factor 2. Position (0,0) corresponds to the stellar object associated with the cometary nebula, star 1 in Table 2. (+) marks the position of IRAS 05274+33.45 and (x) that of the radio continuum source

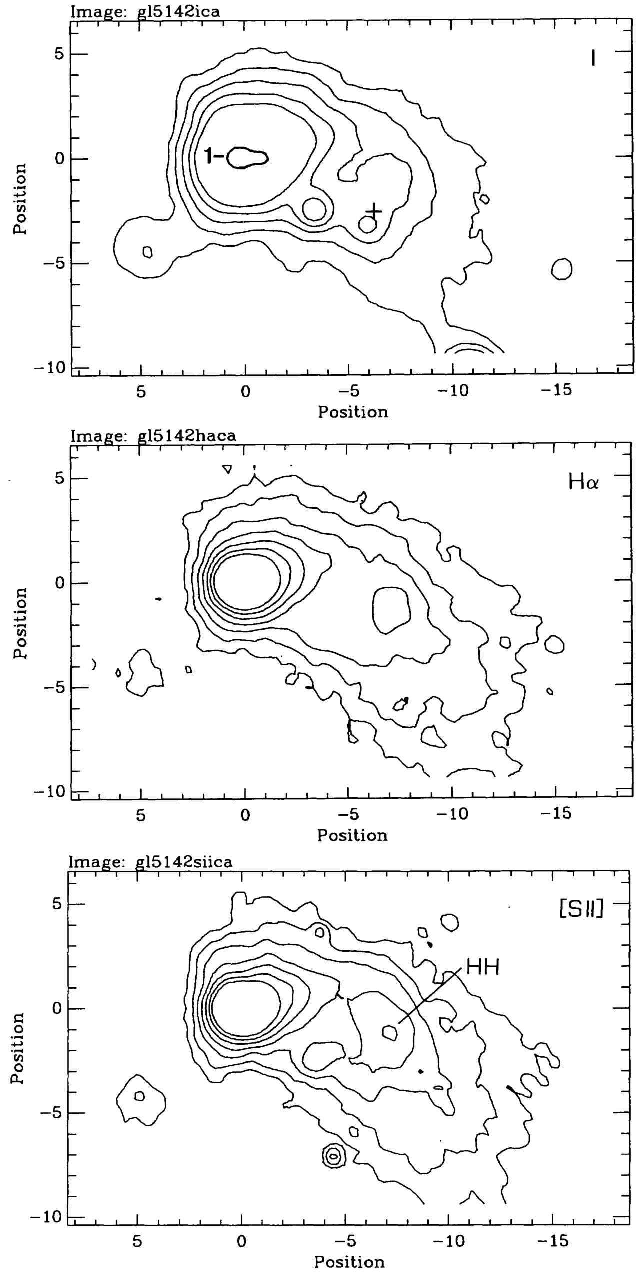

Fig. 3. Detailed I, Hα and [SII] isocontour plots of the AFGL 5142 cometary object. Axes are in arc seconds. Adjacent contours are separated by a factor $2^{1/2}$. Note the very red star close to IRAS 05274+32345 (+) in the I plot and HH 190 in the [SII] plot

3.3. *CB 39*

CB 39 is a small CO core, size 4!5×3!4, listed in the catalogue of Clemens & Barvainis (1988). The core is located close to the IRAS source 05591+1630. Recently, Yun & Clemens (1992) have detected a redshifted outflow associated with this core.

Figure 4 shows the I image obtained at the INT. The only interesting object is a star surrounded by an arc-shaped nebulosity towards the north. The appearance of the object is similar in all the emission line filters; so, we conclude that the nebulosity is reflected light, with no indication of HH emission. The morphology of the system, star and nebulosity, is reminiscent of V 645 Cygni (e.g. Lenzen 1987). The object is located approximately 4′ southwest of the IRAS source, so that any physical association can be excluded.

3.4. *L 1251*

L 1251 is a small, elongated cloud which has been included in some dense core surveys (e.g. Benson & Myers 1989; Zhou et al. 1989). Several IRAS point sources are embedded in the cloud. Schwartz et al. (1988) first discovered a bipolar CO outflow associated with one of them, IRAS 22343+7501. Sato & Fukui (1989) confirmed this outflow and detected a second compact one associated with the IRAS source 22376+7455. Balázs et al. (1992) presented CCD images of the field around IRAS 22343+7501 and reported on the discovery of several HH objects located close to the IRAS source, which they suggested is the driving source. Kun & Prusti (1993) obtained a distance of 300 pc for the dark cloud and found several emission line stars in the area, five of them coinciding with IRAS objects. In this work we present further CCD images of L 1251, concretely of the field around 22376+7455.

Figure 5 shows the INT I image of the field. Many red stars superimposed on a diffuse nebulosity are observed in

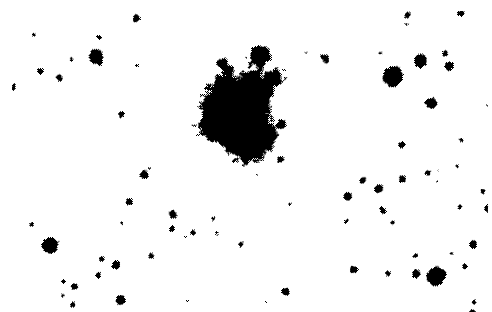

Fig. 4. I image of CB 39. Field size shown is 275″×173 ″

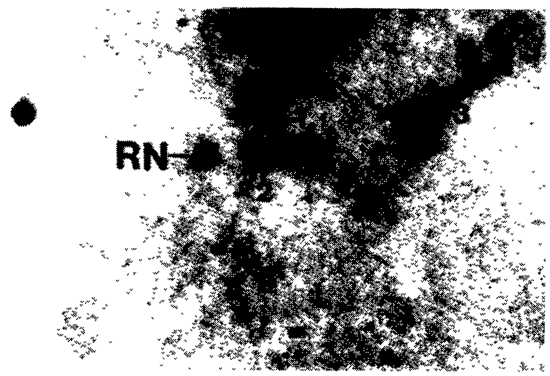

Fig. 5. I image of the field around IRAS 22376+7455 in L1251. The field shown is 6ʹ.1×3ʹ.4 in size. Numbers correspond to stars in Table 3

the field. Coordinates of three nebulous stars are given in Table 3. Star 1 has associated a cometary-like nebulosity oriented towards the north-east. Stars 2 and 3 are also associated with nebulosites. In addition, a very compact and red I nebulosity is detected ≈30″ towards the east of star 2. This nebulosity is called RN in Fig. 5. There is no clear I-counterpart to IRAS 22376+7455, which is located close to star 2 (see also Fig. 6). This star is not very red and we do not know if there is an association between the IRAS object and either star 2 or the reflection nebulosity RN. Figure 6 shows the Calar Alto Hα image of a small field around the IRAS source as an isocontour plot. RN is hardly detected. However, two nebulosities are observed in these images which are not detected in the I image. The nebulosities are also detected in the [SII] image. Therefore, they are pure emission condensations and we identify them as HH objects. In addition, there is a third nebulous object in the field. This object has a faint counterpart in the I image, where it seems to be point-like with a finger of faint nebulosity towards the west. The fact that it is stronger in Hα and [SII] than in I indicates that HH emission is also present in this position. Following the numbering by Reipurth (1994), we call these condensations HH 189A, B and C from North to South. All three HH condensations lie on a straight line pointing towards the nebulous star 1. This result suggests that this star is a candidate for powering the HH emission. However, we can neither exclude that the point-like object embedded in HH 189C is stellar nor that the young object IRAS 22376+7455 is exciting the HH nebulosities.

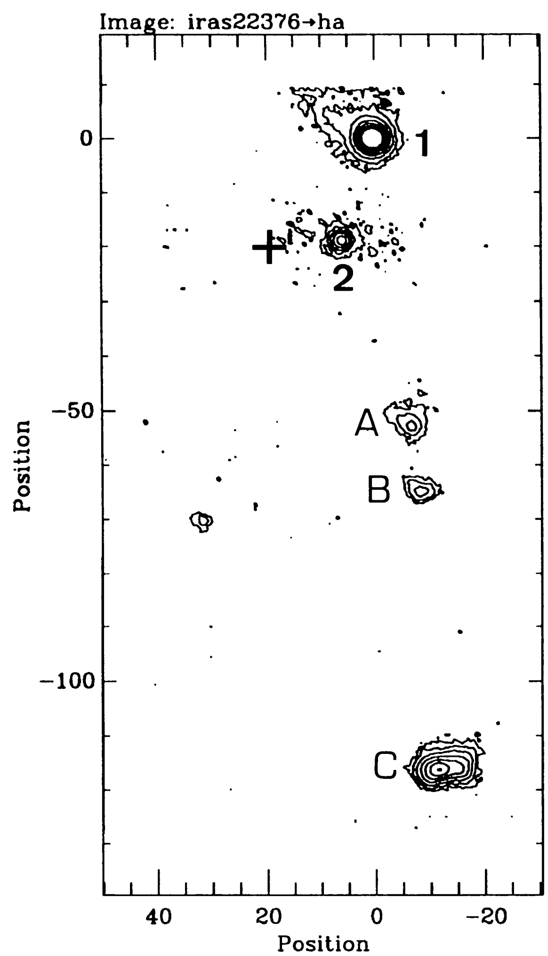

Fig. 6. Hα isocontour plot of the field around 22376+7455 in L1251. Axes are in arc seconds. First contour is 3σ and adjacent contours are separated by a factor 2. The cross denotes the nominal position of IRAS 22376+7455. The condensations A, B and C of HH 189 are marked

Acknowledgements. The Observatorio de Calar Alto is operated jointly by the Max-Planck-Institut für Astronomie (Heidelberg) and the Spanish Comisión Nacional de Astronomía. The Isaac Newton Telescope is operated by the Royal Greenwich Observatory at the Spanish Observatorio Roque de los Muchachos of the Instituto de Astrofísica de Canarias on behalf of the Science and Engineering Research Council of the United Kingdom and the Netherlands Organization for Scientific Research. C.E. and L.F.M. have been supported in part by Spanish Grants DGICYT PB90-0387 and PB91-0007. G.A., R.E., and J.M.T. are partially supported by Spanish Grants PB87-0371 and PB92-0900. GA acknowledges support from an Henri Chrétien award administered by the American Astronomical Society.

References

Balázs L.G., Eisloeffel J., Holl A. et al. 1992, A&A 255, 281

Beichman C.A., Myers P.C., Emerson J.P. et al. 1986, ApJ 307, 378

Benson P.J., Myers P.C. 1989, ApJS 71, 89

Clemens D.P. Barvainis R 1988, ApJS 68, 257

Eiroa C., Lenzen R., Miranda L.F. et al. 1993, AJ 106, 613

Eiroa C., Miranda L.F., Anglada G., Estalella R., Torrelles J.M. 1994, A&A, in press

Estalella R., Mauersberger R., Torrelles J.M. et al. 1993, ApJ 419, 698

Hartigan P., Lada C.J. 1985, ApJS 59, 383

Kun M., Prusti T. 1993, A&A 272, 235

Lenzen R. 1987, A&A 173, 124

Pastor J., Estalella R., Lopez R. et al., A&A 252, 320

Price S.D. 1977, The AFGL Four colour Survey: Supplemental Catalog, Air Force Geophysics Laboratory AFGL-TR-77-0160

Reipurth B. 1994, in preparation

Sato F., Fukui Y. 1989, ApJ 343, 773

Schwartz P.R., Gee G., Huang Y.-L. 1988, ApJ 327, 350

Snell R.L. Huang Y.-L. Dickman R.L. Claussen M.J., 1988, ApJ 325, 853

Torrelles J.M., Eiroa C., Mauersberger R. et al. 1992a, ApJ 384, 528

Torrelles J.M., Gomez J.F., Anglada G. et al. 1992b, ApJ 392, 616

Verdes-Montenegro L., Torrelles J.M., Rodriguez L.F. et al. 1989, ApJ 346, 193

Yun J.L. & Clemens D.P. 1992, ApJ 385, L21

Zhou S., Wu Y., Evans N.J., Fuller G.A., Myers P.C. 1989, ApJ 346, 168